Nitroxide-Labeled Ru(II) Polypyridyl Complexes as EPR Probes of Organized Systems. 3. Characterization of Starburst Dendrimers and Comparison to Photophysical Measurements

M. Francesca Ottaviani,*,† Claudia Turro,‡ Nicholas J. Turro,‡ Stefan H. Bossmann,§ and Donald A. Tomalia⊥

Department of Chemistry, Via G. Capponi 9, 50121 Firenze, Italy

Received: January 10, 1996; In Final Form: May 14, 1996[⊗]

Ruthenium(II) phenanthroline complexes labeled with a nitroxide radical through $-NHCOO(CH_2)-$ and $-O(CH_2)_8O-$ links, RuPT and $RuPC_8T$, respectively, have been utilized as EPR probes to monitor the binding and dynamics of the complexes on the surface of starburst dendrimers (SBDs) of varying size (generations). Analysis of the EPR signals by spectral computation provided structural and dynamic parameters. The cationic probes bind to the negatively charged surface of the half-generation dendrimers (*n*.5-SBDs) through electrostatic interactions, which is consistent with decreased binding upon protonation of the NR_2R' internal groups of the SBDs. The results indicate that there is a fast exchange of RuPT between the *n*.5-SBD surface and the bulk solution and that the probe does not interact with the nonionic full-generation dendrimers (*n*.0-SBDs). The activation energies for the rotational motion of the probes are consistent with their localization in a microheterogeneous environment. $RuPC_8T$ exhibited both hydrophilic and hydrophobic interactions with the anionic *n*.5-SBDs, whereas only hydrophobic interactions were observed with the neutral *n*-SBDs. The $N-O^{\bullet}$ group of $RuPC_8T$ was deduced to be distributed throughout the various hydration layers at the SBD/water interface. A good correlation was found between the rotational mobility of RuPT evaluated by EPR analysis and the translational mobility of $Ru(phen)_3^{2+}$ derived from photophysical measurements, especially for $G = 4.5$ and $G = 5.5$ SBDs.

Introduction

Starburst dendrimers (SBDs) are macromolecules composed of a central core and radially branching units grafted in a symmetrical fashion.[1−5] In particular, the polyamidoamine starburst dendrimers consist of layers (termed generations = *G*) of amidoamine units starting from an ammonia core.[5] The terminal groups of the SBDs, constituting the external surface, may be either amines (full-generation SBDs, termed *n*.0-SBDs) or sodium carboxylates (half-generations, termed *n*.5-SBDs).

Photophysical methods[6−10] and electron paramagnetic resonance (EPR) studies[11−14] have been recently utilized to characterize the surface properties of *n*.5 SBDs. The capability of Ru(II) polypyridyl complexes to probe microheterogeneous anionic surfaces has been demonstrated by photochemical measurements on different organized structures such as alkyl sulfate micelles,[15] polymers,[16] and DNA,[17] as well as the *n*.5-SBDs.[6,7,10] The luminescence properties of bpy (2,2′-bipyridine) and phen (1,10-phenanthroline) complexes of Ru(II) are well-known;[18] both steady-state and time-resolved photoluminescence measurements using these complexes and different cationic quenchers have provided an insight into the surface characteristics of the *n*.5-SBDs, such as changes in surface morphology,[6,8−9] or similarities between the dendrimer surface and the surface of anionic micelles.[7] The photophysical measurements have revealed several aspects of the interaction of Ru(II) complexes with the SBD surface. For instance, it has been found from electron transfer quenching studies that, as the size (generation) of the *n*.5-SBDs increases, the quenching rate constant passes from "bimolecular" when the SBD $G < 4.5$ to "unimolecular" for $G \geq 4.5$ SBDs, and, correspondingly, the exit rates of the probes from the SBD surfaces decrease.[7] These results confirm a change in dendrimer morphology, postulated on the basis of molecular simulations,[19] where the earlier generations ($G < 4.5$) possess open structures and the later generations ($G \geq 4.5$) are characterized by a spherical close-packed structure. The currently accepted paradigm for this system is that the motion of the Ru(II) complexes is slow when bound to the later generation SBDs, whereas the interaction with the surface of the earlier generations is weak and there is fast exchange between the complex on the SBD surface and the bulk solution.

Despite the differences between the two methods and in the probes used, photophysical and EPR studies have provided similar conclusions concerning the nature of the surface properties of the *n*.5-SBDs. For instance, computer-aided analysis of the EPR spectra from both nitroxide radicals[11,12] and paramagnetic metal ions[13,14] confirmed the theoretically computed surface morphology change from earlier to later generations. In addition, EPR analysis and the photophysical studies provide complementary results. The Sano−Tachiya model[20] for diffusion can be utilized in the quenching experiments to evaluate the translational diffusion coefficients of the probes on the dendrimer surface. Conversely, the relaxation mechanism of spin probes with angular spin moment $S = {}^1/_2$, such as nitroxide radicals or Cu(II) ions, is due to the modulation of magnetic tensors by means of rotational diffusion of the molecules.[21] Line shape analysis of the EPR spectra, therefore, leads to the evaluation of the rotational diffusion coefficients. EPR studies also provide structural and dynamic information about the probes and their environments, which aid in the characterization of microheterogeneous structures, such as the interface of the SBD surface and the solvent phase.

The opportunity to combine the photophysical and EPR techniques is possible through nitroxide-labeled Ru(II) polypyridyl complexes, where one of the ligands is a TEMPO-

* Author to whom correspondence should be addressed.
† Department of Chemistry, University of Florence, 50121 Florence, Italy.
‡ Department of Chemistry, Columbia University, New York, NY 10027.
§ Lehrstuhl für Umweltmesstechnik, Universität Karlsruhe, 76128 Karlsruhe, Germany.
⊥ Michigan Molecular Institute, Midland, MI 48640.
⊗ Abstract published in *Advance ACS Abstracts,* July 1, 1996.

S0022-3654(96)00120-7 CCC: $12.00

CHART 1

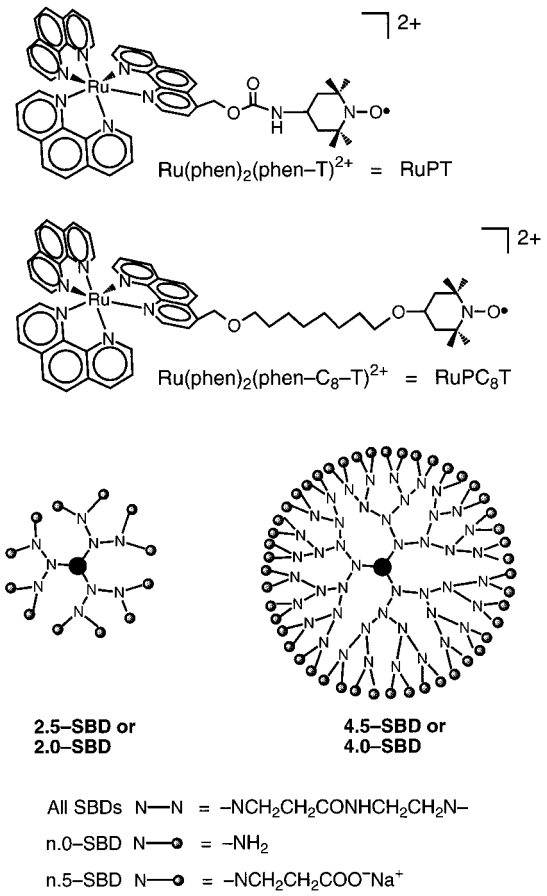

substituted phen (TEMPO = 2,2,6,6-tetramethylpiperidine-*N*-oxyl), tethered to the ligand either through a single $-CH_2-$ group (phen-T)[22] or a $-(CH_2)_8-$ chain (phen-C_8-T).[23] The structures of these probes, termed Ru(phen)$_2$(phen-T)$^{2+}$ and Ru(phen)$_2$(phen-C_8-T)$^{2+}$, referred to as RuPT and RuPC$_8$T, respectively, are shown in Chart 1. RuPT has already successfully demonstrated to be a photoluminescence probe of the surface of polyanionic microheterogeneous systems, such as micelles[22] and DNA.[24] The increasing rotational diffusion coefficients obtained in the EPR for micelles of increasing size are found to correlate extremely well with the translational diffusion coefficients obtained from photophysical studies.[22] RuPC$_8$T differs from RuPT due to the presence of the carbon chain that increases the hydrophilicity of the former probe and provides a further potential anchoring point of the probe to the SBD surface and possibly the SBD interior, which possesses weakly hydrophobic sites. The hydrophobic chain has previously demonstrated to enhance the interaction of radicals at surfaces, also leading to cooperative interaction of the radicals with the macromolecular structure.[11,12,25]

This paper presents a computer-aided EPR analysis of the interactions of RuPT and RuPC$_8$T with *n*.5- and *n*.0-SBDs. The objectives of this work are to (1) analyze the interactions with the dendrimer surface, (2) characterize the surface properties of the dendrimers, and (3) compare the EPR results to those obtained by photophysical means. The rotational diffusion coefficients obtained through the analysis of EPR data are compared to the translational diffusion coefficients extracted from the Sano−Tachiya model for diffusion[20] from the photophysical measurements. In addition, the EPR results from RuPT and RuPC$_8$T were also compared with results previously obtained utilizing the positively charged nitroxide radical 4-(trimethylammonio)-2,2,6,6-tetramethylpiperidine-*N*-oxyl iodide salt (CAT1).[11]

The EPR results presented here have been conducted as a function of SBD generation, pH, temperature, and concentration of both the dendrimers and the probes.

Experimental Section

Full- and half-generation starburst dendrimers (*n*.0-SBDs and *n*.5-SBDs) were synthesized as described previously.[5] All dendrimer solutions were prepared in deionized (Millipore) water and stored at 278 K under nitrogen.

The syntheses of the complexes RuPT and RuPC$_8$T are described elsewhere.[22,23] The concentration of each RuPT solution in water was estimated spectrophotometrically utilizing $\epsilon = 20\,000\ M^{-1}\ cm^{-1}$ at 443 nm.[17c] The RuPT solutions were then diluted as necessary with deionized (Millipore) water. RuPC$_8$T was dissolved in absolute methanol (Fluka) after preparation. The solid product obtained following solvent evaporation was weighed, thus permitting preparation of aqueous solutions at fixed concentrations, which were diluted as necessary. The concentration of the probes used in all the experiments was 0.1 mM.

The probe and dendrimer solutions were mixed in the appropriate amounts, and the EPR spectra were recorded immediately after sample preparation. Aging of the solutions lead to a progressive decrease in EPR signal intensity, especially at high pH, due to radical degradation. The effect of aging on the probe mobility will be discussed in the Results and Discussion.

All the reported EPR spectra were recorded on a Bruker 200D interfaced to a PC outfitted with a Stelar software system. Temperature control was achieved with a Bruker 100/700T unit.

The variation of pH was accomplished by adding appropriate amounts of HCl (Merck, used as received) from a 1.2 M stock solution. The pH was measured with a Sentron-2001 pH meter, kindly provided by Prof. M. Mascini, University of Florence, equipped with a microelectrode to permit the measurement of small volumes (0.2 mL).

Results and Discussion

SBD Generation Dependence. Representative experimental (full lines) EPR spectra of RuPT (0.1 mM) in the presence of 2.5, 4.5, and 6.5 generation dendrimers ([SBD$-$COO$^-$] = 0.3 M) recorded at 293 K and pH = 8.5 are shown in Figure 1. The computed spectra are superimposed as dashed lines to the experimental patterns. The spectra were calculated utilizing a well-established procedure developed by Schneider and Freed.[26] The main input parameters used in the calculation of the spectra are the following:

(i) The principal components of the **g** and $\mathbf{A_N}$ tensors for the Zeeman (electron spin-magnetic field) and hyperfine (electron spin-nuclear spin) coupling, respectively. The **g** principal components previously used for RuPT in micellar and DNA systems, $g_{xx}, g_{yy}, g_{zz} = 2.0097, 2.0063, 2.0035$,[22,23] were utilized. The $\mathbf{A_N}$ components producing the best fit to the experimental data and the computed line shapes for most of the spectra in this work were $A_{xx}, A_{yy}, A_{zz} = 6.8$ G, 7.5 G, 37.3 G, respectively.

(ii) The main components of the rotational diffusion tensor **D**. In the case of axial symmetry the main components of the diffusion coefficient are $D_{||}$ and $D_{\perp}$, where $D_{\perp}$ is the most relevant parameter for the analysis of the spectra. The calculation also includes the tilt angle between the main rotational diffusion axis and the main magnetic axis. The main rotational axis of RuPT is defined in the direction through the links between the nitroxide group and the RuP complex, whereas the

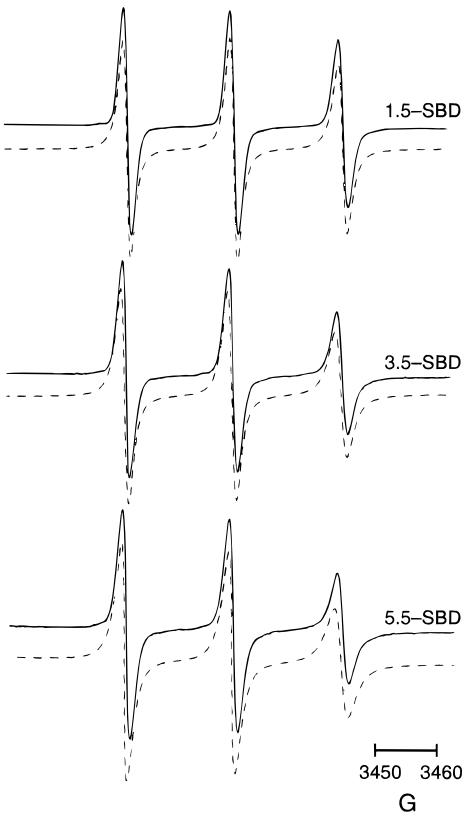

Figure 1. Experimental (full lines) EPR spectra of RuPT (0.1 mM) in the presence of 2.5-, 4.5-, and 6.5-SBDs ([SBD−COO$^-$ = 0.3 M), recorded at 293 K and pH = 8.5. The computed spectra are superimposed as dashed lines to the experimental patterns.

TABLE 1: Parameters Used for the Computation of the EPR Spectra of RuPT in *n*.5-SBD Solutions (Figure 1), with g_{xx}, g_{yy}, g_{zz} = 2.0097, 2.0063, 2.0035 and A_{xx}, A_{yy}, A_{zz} = 6.8 G, 7.5 G, 37.3 G.

generation	$D_\perp$ (s^{-1})[a]	tilt[b]	$1/T_{2,0}$ (G)
2.5	1.7×10^9	/	0.8
4.5	2.6×10^8	60°	1.0
6.5	1.7×10^8	70°	1.2

[a]Brownian rotational diffusion model of motion: $D_\perp = 1/(6\tau_\perp)$; $D_\parallel = 3D_\perp$. [b]Tilt angle between the diffusion rotational frame and the magnetic frame.

principal magnetic axis is in the direction of the p_z orbital of the N atom containing the unpaired electron. $D_\perp$ and the tilt angle for the spectra in Figure 1 are listed in Table 1.

(iii) The intrinsic line width $1/T_{2,0}$, which accounts for inhomogeneous broadening and of hyperfine lines. The parameters utilized in the computation are listed in Table 1.

Despite the simple line shape of the spectra in Figure 1, each parameter accounts for different peculiarities in the spectra and, therefore, may be evaluated with rather good accuracy (5%). For instance the increase in the tilt angle mainly produces an increase in the height of the first hpf line with respect to the other two lines, whereas the decrease in $D_\perp$ accounts for the decrease in the height of the third hpf line with respect to the other two.

The values were consistent with the following conclusions: (i) the mobility of the probe ($D_\perp$) decreased with an increase in the dendrimer size and (ii) the increase in dendrimer size led to a progressive shift of the rotational axis toward the N−O direction, probably due to the higher strength of interaction of RuPT with the dendrimer surface with increasing dendrimer size.

The correlation time for motion in a series of measurements on the same radical under the same experimental conditions

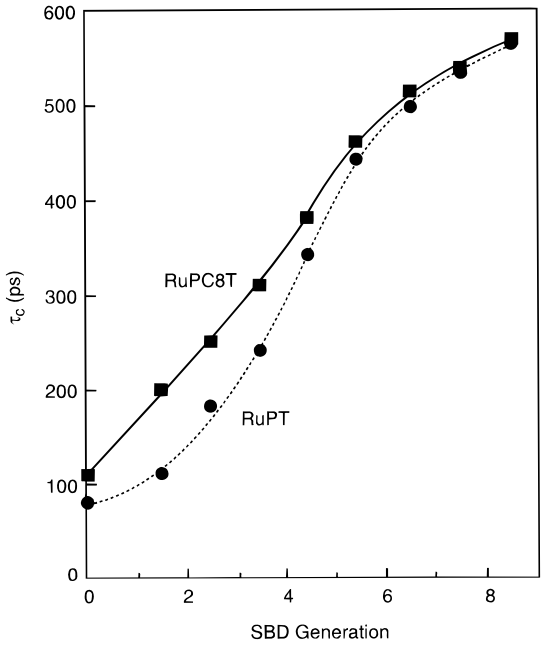

Figure 2. Plots of τ_c, evaluated from the EPR spectra at 293 K and pH = 8.5 (eq 2), as a function of *n*.5-SBD generation ([SBD−COO$^-$ = 0.3 M for all generations) for RuPT and $RUPC_8T$.

were evaluated by utilizing the following simplified formulas for τ_B and τ_C (accuracy 5%):

$$\tau_B = B^*\Delta H_o[(h_o/h_1)^{1/2} - (h_o/h_{-1})^{1/2}] \quad (1)$$

$$\tau_C = C^*\Delta H_o[(h_o/h_1)^{1/2} + (h_o/h_{-1})^{1/2} - 2] \quad (2)$$

where h_i are the peak heights and $B^* \approx C^* \approx 5.7 \times 10^{-10}$, which is comparable to the typical value $B^* \approx C^* \approx 6.5 \times 10^{-10}$ used for nitroxide radicals in aqueous solution.[27] In addition, $B^* \approx C^* \approx 5.7 \times 10^{-10}$ also provided correlation times for motion that were in good agreement with the values obtained by means of the computational procedure. Figure 2 shows the variation of for RuPT and $RuPC_8T$ as a function of *n*.5G dendrimer generation ([SBD−COO$^-$] = 0.3 M for all generations, T = 293 K, and pH = 8.5).

Analysis of the spectra by means of line shape computation indicates that at least the two parameters reported in Table 1, $D_\perp$ and the tilt angle, should be evaluated in order to define the mobility conditions of the probes in the presence of SBDs. The use of the eq 1 for the evaluation of the correlation times for motion, τ_B and τ_C, permitted an easier comparison of the motional conditions in the series of samples at increasing dendrimer generation for each probe. Figure 2 shows the variation of $\tau_c = (\tau_B\tau_C)^{1/2}$ (evaluated utilizing eq 1 at 293 K and pH = 8.5) for RuPT and $RUPC_8T$ as a function of *n*.5G dendrimers ([SBD−COO$^-$] = 0.3 M for all generations). In analyzing this graph, the following issues should be noted: (a) the size of the probe molecules (about 18 Å diameter for Ru(phen)$_3^{2+}$) is comparable to the size of SBDs of generations 3.5−4.5; (b) the opposite charge of the probes (positive) and the half-generation dendrimer surface (negative) should assist in electrostatic binding; (c) the ratio between the concentration of the surface carboxylate groups and the concentration of the probe was maintained constant for all generation: [SBD−COO$^-$]/[probe] = 3000; (d) the density of SBD−COO$^-$ groups increases, whereas the curvature of the surface decreases, with the increase in generation. In addition, the change in morphology from earlier to later generations (at G = 4.5) corresponds

to passage from open to closed, more packed structures; thus, (e) the interaction between the ruthenium complexes and the surface of the SBDs is enhanced by hydrophobic forces due to the presence of the phen groups and of the long $-(CH_2)_8-$ chain in the $RuPC_8T$ probe.

From point a it would be expected that the interactions of the probes with the SBD surface would lead to a significant perturbation of the dendrimer surface, especially for $G < 4.5$. However, a large variation in the mobility of RuPT was found between $G = 3.5$ and $G = 5.5$. Since the number of surface COO^- groups was maintained constant in all the measurements (point c), the increase in τ_c with generation is not related to the number of COO^- groups. The correlation times of our probes in fast motion conditions indicate that the fast rotation is about the main rotational axis of the radical (along the N−O bond) through the linker to the ruthenium complex bound to the SBD surface. Thus, the increase in τ_c from earlier to later generations might be ascribed to the larger charge density and the lower curvature of later generations, since the positively charged probe is bound more tightly to the surface of the later generation dendrimers. A sharp variation in the lifetime of excited $Ru(bpy)_3^{2+}$ at the SBD surface has been previously found upon passing from earlier to later generation *n*.5-SBDs,[6] which is in qualitative agreement with the EPR results for RuPT shown in Figure 2. Similarly, the intrastarburst quenching of $*Ru(phen)_3^{2+}$ by methylviologen has been found to pass from bimolecular, for earlier generation dendrimers, to unimolecular in the later generation SBDs.[7]

It is of interest that the correlation time of RuPT for 3.5-SBD and for sodium alkyl sulfate micelles of comparable size (C_7 and C_8) were similar, with $\tau_c \approx 250$ ps.[22] However, the increase in τ_c with the increase in micellar size is much larger than that observed with dendrimer generation, even if the size of the micelles was smaller (radius ranging from 17 to 33 Å in the range of C_8 to C_{16}) than that of the dendrimers (radius ranging from 14 to 74 Å in the range of 1.5 to 8.5 G). Therefore, as was previously established, the binding of cationic Ru(II) complexes to the surface of the negatively charged alkyl sulfate micelles is stronger than to the carboxylate groups on the *n*.5-SBD surfaces.[7,11,28] Also the anisotropy of motion and the diffusion tilt angles were larger for RuPT interacting with sodium alkyl sulfate micelles than with dendrimers.[22]

The graph in Figure 2 also shows the variation of mobility for $RuPC_8T$ as a function of SBD generation. As suggested in point e, the presence of the hydrophobic chain should enhance the interaction of the probe with the surface or with the hydrophobic SBD interior. However, it is noteworthy that this enhancement, corresponding to the increase in τ_c for $RuPC_8T$ with respect to RuPT, was more significant for the earlier generations than for later ones. Indeed, the mobilities of $RuPC_8T$ and RuPT were nearly identical in the presence of the later generation dendrimers. This effect probably arises from the available internal, partially hydrophobic sites in the open structure of the earlier generation SBDs. Conversely, the closed, packed structure of the later generation dendrimers prevented the penetration of the hydrophobic $-(CH_2)_8-$ chain to permit the interaction with the hydrophobic internal NCH_2CH_2C groups. It has been suggested that the hydrophobic chain attached to a positively charged nitroxide, CAT*n* ($n = 1$, 4, 8, 12, 16), provided an "anchor", which binds the probe to the internal hydrophobic groups of the SBDs.[11] However, the nitroxide (TEMPO) was mainly localized in the hydration layers of the dendrimer surface, since the hyperfine coupling constant $\langle A_N \rangle$, which is a measure of environmental polarity, was practically unaffected by the addition of *n*.5-SBDs of various generations. The cationic CAT*n* molecules showed a trend opposite to that of $RuPC_8T$ when interacting with the dendrimers of various generations, where the interaction between the hydrophobic chain and the dendrimer became stronger as the SBD generation increased. In this regard we must consider that the phen ligands may play a relevant role in the hydrophobic interactions with the dendrimer.

TABLE 2: Main Parameters Obtained from the Analysis of the EPR Spectra of RuPT and $RuPC_8T$ in *n*.0-SBD Solutions

	RuPT		$RuPC_8T$	
generation	τ_c (ps)	$\langle A_N \rangle$ (G)	τ_c (ps)	$\langle A_N \rangle$ (G)
0.0	80	17.02	110	16.97
2.0	115	16.85	310	16.78
4.0	90	16.88	260	16.86
6.0	80	16.95	230	16.91

The variation of the hyperfine coupling constant $\langle A_N \rangle$ with SBD generation is nearly negligible for both RuPT and $RuPC_8T$. However, a small decrease in $\langle A_N \rangle$ for $RuPC_8T$ (16.85 ± 0.03 G) compared to RuPT (17.00 ± 0.03 G) was found in the presence of SBDs. This finding can be attributed to a slightly lower environmental polarity of the TEMPO radical in $RuPC_8T$ than in RuPT, although the magnitude of $\langle A_N \rangle$ in both cases is consistent with the localization of the radical moiety in the hydration layers of the SBD surface.

The parameters obtained from the analysis of the EPR spectra of the probes (0.1 mM) as a function of full generation of the dendrimers ($[SBD-COO^-] = 0.3$ M, 293 K, pH = 9) are listed in Table 2. The parameters reported in Table 2 lead to the following conclusions:

(i) The interaction of RuPT with full-generation dendrimers was almost negligible, since the parameters changed slightly from pure RuPT solution to the solutions in the presence of the dendrimers.

(ii) Full-generation SBDs showed an opposite variation of τ_c as a function of generation when compared to the half-generation SBDs.

The above findings indicate that the interaction between the probes and the *n*.0-SBDs is predominantly hydrophobic in nature. The surface of the full-generation *n*.0-SBDs at pH 9 is mostly uncharged (NH_2 groups, Chart 1), and therefore, electrostatic interactions are not significant. The less polar sites, which are part of the internal SBD structure, are more exposed in the earlier generations compared to the later ones. Hence, both the mobility and the environmental polarity of the probes diminished in the presence of the earlier generation dendrimers, especially in the case of $RuPC_8T$, due to the presence of the hydrophobic $-(CH_2)_8-$ chain.

pH Dependence of the EPR Spectra. Figure 3 shows the variation in the correlation time for motion, τ_c, evaluated from the EPR spectra of RuPT (0.1 mM) at 293 K utilizing eq 1 as a function of pH in the presence of 3.5-SBD and 5.5-SBD ($[SBD-COO^-] = 0.3$ M). 3.5-SBD was selected as representative of the earlier SBD generations, whereas 5.5-SBD was chosen to represent the behavior of the later generation dendrimers. $RuPC_8T$ exhibited similar results to those observed for RuPT. The results reported in the previous section were obtained from the analysis of EPR spectra at pH = 8.5. Above this pH, it was necessary to perform the EPR measurements within 10 min of sample preparation, to avoid fast degradation of the system, manifested as a decrease in signal intensity and an increase in radical mobility. The degradation was more evident in the later generations than in the earlier SBDs. The values of τ_c reported in Figure 3 indicate that τ_c of RuPT in the presence of 3.5-SBD increased up to pH 10.5 and then abruptly decreased with further small increases in pH. For 5.5-SBD

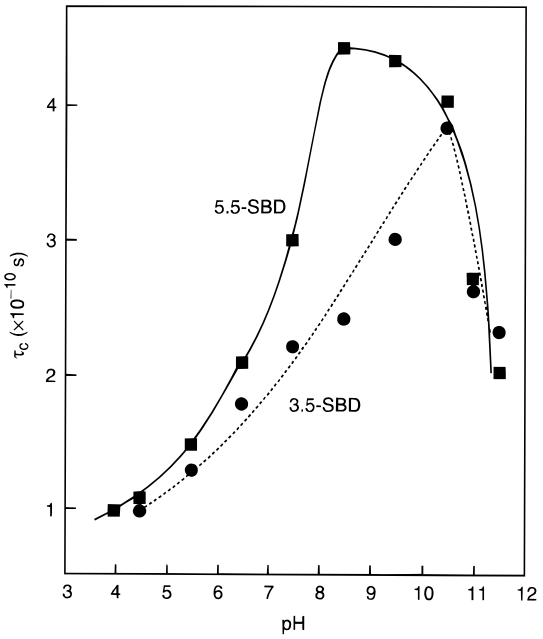

Figure 3. Variation of the correlation time for motion (eq 1) from the EPR spectra at 293 K, as a function of pH for 3.5-SBDs and 5.5-SBDs ([SBD−COO^-] = 0.3 M) solutions containing RuPT (0.1 mM).

solutions, the τ_c of RuPT also increased with increasing pH, but at pH > 8.5, τ_c started decreasing slowly up to pH 10.5 and quickly at pH > 10.5. The graph does not show data obtained at pH ≤ 3.5, since the values of τ_c were not reproducible in subsequent EPR experiments, even for freshly prepared samples.

The analysis of the variation of τ_c as a function of pH was therefore confined to the range 3.5 < pH < 9 for 5.5-SBD and 3.5 < pH < 11 for 3.5-SBD. For both 3.5- and 5.5-SBDs the mobility decreased as the pH increased. However, 5.5-SBD solutions showed a marked increase in τ_c (from 300 to 440 ps) between pH 7.5 and 8.5, whereas a similar increase (from 300 to 380 ps) was observed for 3.5-SBD between pH 9.5 and 10.5 (Figure 3). A recent study has reported that the deprotonation of the $NR_2R'H$ groups closest to the surface in 5.5-SBD occurs at pH > 7.[14] Conversely, the deprotonation of the $NR_2R'H$ groups closer to the surface in 3.5-SBD takes place at pH > 8. This result explains the variation of τ_c in Figure 3. A marked increase in τ_c, which corresponds to a stronger interaction of the probe with the SBD surface, occurs only when the SBD internal surface is not protonated. Thus, the driving force for the initial interaction of the cationic probe to the *n*.5-SBD surface is electrostatic in nature, centered on the attraction between the SBD−COO^- groups and the positively charged probes.

The variation of $\langle A_N \rangle$ was negligible in all the pH ranges investigated. No interactions with full-generation SBDs were found at pH < 9, due to the protonation of the surface amino groups. At pH > 9.5, the stability of the probe/*n*.0-SBD systems strongly decreased.

Mobility as a Function of Temperature. Figure 4 shows the variation of log(τ_c) as a function of *T* for RuPT and $RuPC_8T$ (0.1 mM) at pH = 8.5 for 3.5-SBD (Figure 4a) and 6.5-SBD (Figure 4b) with [SBD−COO^-] = 0.3 M. For comparison, the plots of log(τ_c) vs *T* for the nitroxide CAT1 are also shown in the graph. The analysis of the plots in Figure 4, for the regions in which the differences in τ_c were well beyond the error margin in the evaluation of τ_c (accuracy = 5%), addresses the following issues:

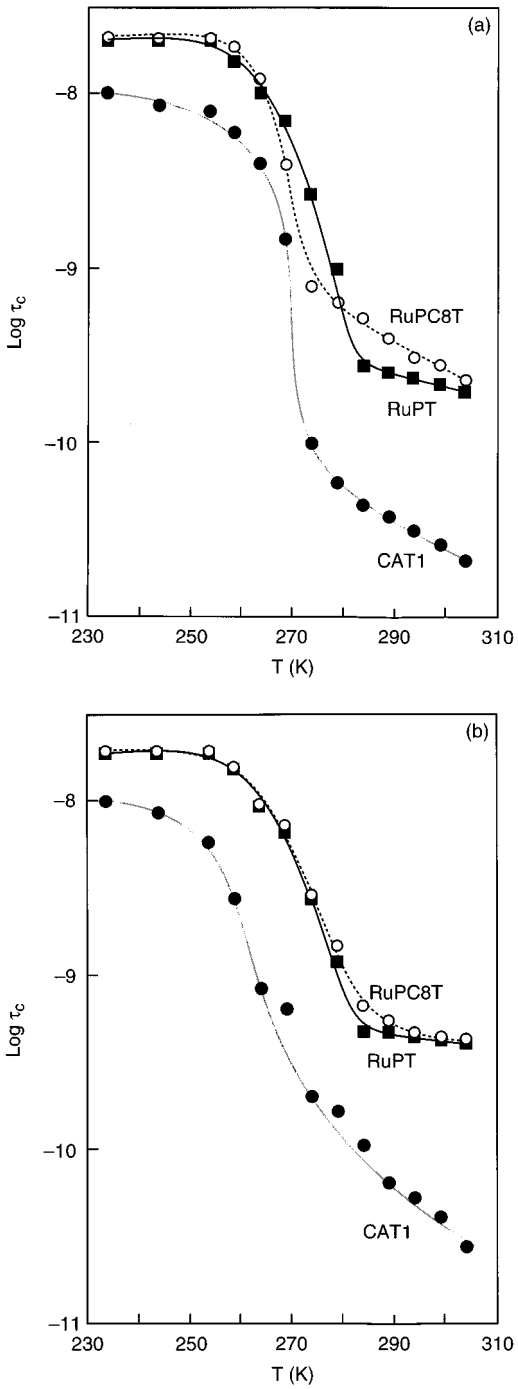

Figure 4. Variation in log(τ_c) as a function of *T* for RuPT and $RuPC_8T$ (0.1 mM) at pH = 8.5 in the presence of (a) 3.5-SBDs and (b) 6.5-SBDs ([SBD−COO^-] = 0.3 M). As a comparison, the plot of log(τ_c) vs *T* for CAT1 is also reported.

(1) The mobility of CAT1 is higher than that of both RuPT and $RuPC_8T$ in the temperature range investigated.

(2) At both $T \geq 283$ K and $T \leq 263$ K, the trend for the mobilities of the three probes is $\tau_c(\text{CAT1}) \ll \tau_c(\text{RuPT}) \leq \tau_c(RuPC_8T)$, which is consistent with the evidence that (i) the electrostatic interaction with the negatively charged SBD surface is stronger for Ru^{2+} complexes than for the single-charged cationic CAT1 and (ii) the hydrophobic $-(CH_2)_8-$ chain in $RuPC_8T$ enhances the interaction with the SBD surface. As discussed earlier for Figure 2, the decrease in mobility from RuPT to $RuPC_8T$ was mainly observed with the earlier generations (Figure 4a for 3.5-SBD).

(3) Interestingly, for 3.5-SBD (Figure 4a), a reverse trend is observed, where $\tau_c(RuPC_8T) < \tau_c(\text{RuPT})$ in the range 263 K

TABLE 3: Values of Correlation Times for Motion of RuPT and $RuPC_8T$ Containing 3.5-SBD at Various Concentrations and at Selected Times after Preparation

		τ_c (ps)	
[SBD−COO^-] (M)	aging	RuPT	$RuPC_8T$
0.30	fresh	240	310
0.15	fresh	170	240
0.08	fresh	90	190
0.30	1 day	200	270
0.30	2 days	140	220
0.30	3 days	110	180

TABLE 4: Values of Correlation Times for Motion of RuPT and $RuPC_8T$ Containing 6.5-SBD at Various Concentrations and at Selected Times after Preparation

		τ_c (ps)	
[SBD−COO^-] (M)	aging	RuPT	$RuPC_8T$
0.30	fresh	490	510
0.15	fresh	250	430
0.08	fresh	130	330
0.30	1 day	320	470
0.30	2 days	190	300
0.30	3 days	120	250

$< T <$ 283 K. This effect can be explained by a slower quenching in mobility of the water layers surrounding the nitroxide moiety of $RuPC_8T$ when compared to RuPT. It is possible that the anchoring of $RuPC_8T$ through interactions of the $-(CH_2)_8-$ chain with internal hydrophobic sites of the SBD structure precludes the rapid exchange of the probe bound to the dendrimer and the bulk solution.

(4) The slopes at higher temperature are different for the various samples, which reflects the variation in activation energies for rotational motion, ΔE^*. From the Arrhenius plots, $-\log(\tau_c)$ vs $1/T$, it was found that ΔE^* for RuPT in the presence of 3.5- and 6.5-SBDs is 2.8 and 1.5 kcal/mol, respectively. The value of ΔE^* for $RuPC_8T$ bound to 3.5-SBD was found to be 6.6 kcal/mol; however, the value for $RuPC_8T$ in 6.5-SBD was not measurable owing to the nonlinearity of $\log(\tau_c)$ as a function of $1/T$. We hypothesize a different distribution of the radical groups of $RuPC_8T$ in the various hydration layers at various temperatures, which also accounts for the slow quenching in the mobility of the probes and gives rise to the nonlinearity of the plot.

Conversely, it is important that a low ΔE^* value was found for RuPT in the presence of the SBDs. Such low values are typical of radicals in microheterogeneous environments, such as radical solutions adsorbed onto porous supports.[29] The TEMPO moiety of RuPT is therefore localized in the hydration layers of the SBD surface, and although there is a rapid exchange between the surface layers and more external water layers, the radicals seem to be partially protected from external effects, such as collisions which would lead to the variations in the $\log(\tau_c)$ vs $1/T$ plots.

Effect of Concentration and Aging. The dilution of the dendrimers solutions led to an increase in mobility of the radicals. A similar effect was observed for the aging of the samples. The values of the correlation times for motion evaluated (eq 1, 293 K) for samples containing SBDs at various concentrations and at selected times after preparation are listed in Tables 3 and 4 for 3.5- and 6.5-SBDs, respectively. The mobility of RuPT in very dilute SBD solutions or in aged (more than 3 days) samples showed almost no interaction with the SBDs. Therefore, τ_c approaches the value found for RuPT in water, 80 ps. Conversely, $RuPC_8T$ was found to still be bound to the SBDs to some extent even at the highest dilutions or in aged samples.

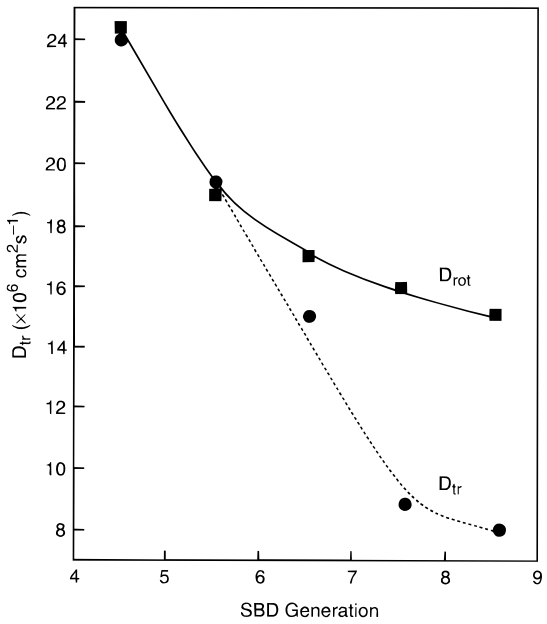

Figure 5. Estimated translational diffusion coefficient, D_{tr}, for $Ru(phen)_3^{2+}$ (refs 7, 10, and 20) and scaled rotational diffusional coefficients, D_{rot}, of RuPT as a function of generation.

The equilibrium between the probe in solution and the probe at the surface is given by

$$(\text{probe})_{aq} + \text{SBD} \leftrightarrows (\text{probe})-\text{SBD} \qquad (3)$$

where lower [SBD] leads to lower [(probe)−SBD] and higher [$(\text{probe})_{aq}$]. The different behavior between RuPT and $RuPC_8T$ again resides in the effect of the $-(CH_2)_8-$ chain, which binds to the SBD internal hydrophobic sites and prevents the radicals from fast exchange with the bulk solution.

Comparison between Photophysical and EPR Measurements. Dynamic quenching experiments of photoexcited $Ru(phen)_3^{2+}$ with cationic species lead to the evaluation of the quenching rate constants of the probe by methylviologen or $Co(phen)_3^{2+}$ bound to the negatively charged *n*.5-SBD surface.[7,10] The Sano−Tachiya model for diffusion permits the evaluation of the coefficients for translational diffusion, D_{tr}, on the surface of the different sized dendrimers.[20] The values of D_{tr} on SBDs of generations ranging from 4.5 to 8.5 are presented as open circles in Figure 5. Values of D_{tr} at lower generations could not be evaluated in a similar way as for $G > 4$, since the quenching reaction at the surface of earlier generation SBDs was found to be bimolecular in nature due to the fast exchange of the probe between the SBD surface and the bulk solution.[7] The decrease in D_{tr} with increasing generation shows the progressive slower translational mobility of the probe as the size of the dendrimers increases. This result is consistent with the EPR experiments wherein a lower rotational mobility of RuPT is found with the increase in generation (Figure 2). To compare the results from photophysical and EPR experiments, the graph in Figure 5 also presents, as open squares, the values of the rotational diffusion coefficient of RuPT, $D_{rot} = 1/(6\tau_c)$, which have been normalized by a constant coefficient in order to have almost coincident numerical values of D_{tr} and D_{rot} for the lower generations in the graph. We have to consider that the comparison holds only in the case where both the translational and rotational mobilities refer to the entire probe. This is not obvious from the rotational mobility, usually associated with the local dynamics of the nitroxide, since the TEMPO group is not rigidly linked to the RuP complex. However, the main rotational axis is defined in the direction through the links

CHART 2

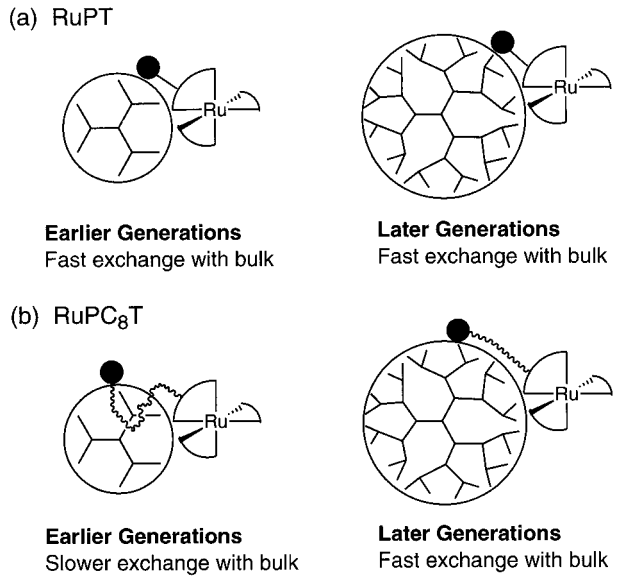

between the nitroxide group and the RuP complex. Therefore, we assume that the variations in the rotational mobility of the nitroxide group reflect the variations in the strength of the interaction of the Ru complex with the dendrimer surface. The same holds for the translational mobility. The points overlap for 4.5 and 5.5 G, whereas the rotational motion becomes "faster" with respect to the translational motion for higher generations. This discrepancy may be due to the effect of O_2 on the photophysical measurements, since it is believed that the concentration of O_2 at the surface of the SBDs, where the Ru(II) complexes bind, is lower than in the bulk solution.[10] The lower oxygen concentration at the SBD surface leads to longer emission lifetimes, which in turn modify the value of D_{tr}. Since O_2 does not affect the EPR signal of nitroxides, the decreased oxygen concentration on the SBD surface may account for the difference between D_{tr} and D_{rot}, especially with the higher generation SBDs. A good parallel is found between the variations of the two diffusional coefficients as a function of the dendrimer size. This correspondence is evidence that the rotational and the translational mobilities of the probe are influenced in a similar manner by the binding of the probe to the SBD surface. Therefore, the results from the EPR probes are in agreement with and support the results obtained from photophysical experiments.

Conclusions

Ruthenium(II) phenanthroline complexes labeled with a nitroxide radical through a $-NHCOO(CH_2)-$ link (RuPT) or a $-O(CH_2)_8-$ link ($RuPC_8T$) were utilized as EPR probes for the characterization of half- and full-generation starburst dendrimers, namely *n*.5-SBDs and *n*.0-SBDs, respectively.

The EPR spectra of RuPT and $RuPC_8T$ were recorded and analyzed by computer simulation, at various pH values and temperature, in the presence of *n*.5-SBDs and *n*.0-SBDs of different sizes (generations). The results and conclusions from these experiments are pictorially shown in Chart 2. Chart 2a shows that the cationic RuPT electrostatically interacts with the oppositely charged surface of *n*.5-SBDs. The increase in the correlation times for rotational motion with increasing SBD generation indicates that the probe is bound more strongly to the surface of later generation dendrimers ($G > 4.5$). This result is in good agreement with those obtained for the interaction of RuPT with sodium alkyl sulfate micelles of different sizes.[22] Analysis of the mobility as a function of pH shows that the electrostatic interaction takes place only under the condition that the negative charge of the *n*.5-SBD surface is not "neutralized" by the protonation of the internal NR_2R' groups, which occurs at pH < 8.5 for 5.5-SBD and at pH < 10.5 for 3.5-SBD. The results as a function of temperature are consistent with the localization of the radical in microheterogeneous environments, partially protected from external agents, but in fast exchange with the bulk solution. Only very modest changes in the hyperfine coupling constant $\langle A_N \rangle$ were observed upon addition of SBDs to aqueous solutions. This result is indicative of the localization of the nitroxide moiety in the Gouy−Chapman layer surrounding the *n*.5-SBDs. The RuPT probe does not interact with full generation dendrimers. However, the RuPT−*n*.5-SBD interaction is lost at high pH (>10.5), in dilute SBD solutions, and upon aging of the samples.

Chart 2b shows that both hydrophilic (electrostatic) and hydrophobic interactions occur between $RuPC_8T$ and the SBDs. The hydrophobic interactions between the phen-C_8 moiety and the internal hydrophobic SBD sites (probably the less polar $NHCH_2CH_2C$ groups) decrease the mobility of this probe compared to RuPT. These interactions only occur in the $RuPC_8T$/*n*.0-SBD system. Furthermore, the hydrophobic interactions are more effective in the earlier generations of both the half-generation ($G \leq 4.5$) and the full-generation ($G \leq 4$) dendrimers. The open external configuration of the earlier generation SBDs is proposed to favor the penetration of the $-(CH_2)_8-$ chain into the interior of the SBD structure. The results as a function of T show that $RuPC_8T$ is distributed among the various hydration layers at the SBD surface in slow exchange with the bulk solution. It is hypothesized that the phen-C_8 anchors the probe at the SBD internal structure.

The results and conclusions from these experiments were mutually supportive of the results obtained from the photophysical properties of $Ru(phen)_3^{2+}$ in the presence of *n*.5-SBDs.[7,10] A correspondence was found between the translational diffusional coefficient, D_{tr}, from photophysical measurements[20] and the rotational diffusional coefficient, D_{rot}, evaluated from EPR spectral analysis, especially for the lower generations (4.5−5.5).

Our EPR probes therefore nicely serve to compare and support the results obtained from photophysical experiments and provide further insight to the knowledge of the surface properties of SBDs.

Acknowledgment. N.J.T. thanks the AFOSR and NSF for their generous support. D.A.T. thanks the New Energy and Development Organization (NEDO) of the Ministry of International Trade and Industry of Japan (MITI) for its generous support and certain critical synthetic efforts. M.F.O. thanks the Italian Ministero Università e Ricerca Scientifica e Tecnologica (MURST) and the Italian Consiglio Nazionale delle Ricerche (CNR) for financial support. C.T. thanks the Jane Coffin Childs Memorial Fund for Medical Research for a fellowship. This investigation has been aided by a grant from The Jane Coffin Childs Memorial Fund for Medical Research.

References and Notes

(1) *Advances in Dendritic Macromolecules*; Newkome, G. R., Ed; JAI Press: Greenwich, CT, 1993.

(2) (a) Krohn, K. Starburst Dendrimers and Arborols. *Org. Synth. Highlights* **1991**, 378. (b) Amato, L. Trekking in the Molecular Forest. *Science News* **1990**, *138*, 298.

(3) (a) Newkome, G. R.; Moorefield, C. N.; Baker, G. R.; Johnson, A. L.; Behera, R. K. *Angew. Chem., Int. Ed. Engl*. **1991**, *30*, 1176. (b) Newkome, G. R.; Moorefield, C. N.; Baker, G. R.; Saunders, M. J.; Grossman, S. H. *Angew. Chem., Int. Ed. Engl*. **1991**, *30*, 1178. (c) Newkome,

G. R.; Young, J. K.; Baker, G. R.; Potter, R. L.; Audoly, L.; Cooper, D.; Weis, C. D. *Macromolecules* **1993**, *26*, 2394.

(4) (a) Kim, Y. H.; Webster, O. W. *J. Am. Chem. Soc.* **1990**, *112*, 4592. (b) Hawker, C. J.; Wooley, K. L.; Fréchet, J. M. J. *J. Chem. Soc., Perkin Trans. 1* **1993**, 1287. (c) Fréchet, J. M. J. *Science* **1994**, *263*, 1710. (d) Jansen, J. F. G. A.; deBrabander-Van de Berg, E. M. M.; Meijer, E. W. *Science* **1994**, *266*, 1226.

(5) (a) Tomalia, D. A.; Baker, H.; Dewald, J.; Hall, M.; Kallos, G.; Martin, S.; Roeck, J.; Smith, P. *Polym. J. (Tokyo)* **1985**, *17*, 117. (b) Tomalia, D. A.; Baker, H.; Dewald, J.; Hall, M.; Kallos, G.; Martin, S.; Roeck, J.; Smith, P. *Macromolecules* **1986**, *19*, 2466. (c) Tomalia, D. A.; Berry, V.; Hall, M.; Hedstrand, D. M. *Macromolecules* **1987**, *20*, 1164. (d) Tomalia, D. A.; Hall, M.; Hedstrand, D. M. *J. Am. Chem. Soc.* **1987**, *109*, 1601. (e) Padias, A. B.; Hall, H. K.; Tomalia, D. A.; McConnell, J. R. *J. Org. Chem.* **1987**, *52*, 5305. (f) Wilson, L. R.; Tomalia, D. A. *Polym. Prepr. (Am. Chem. Soc. Div., Polym. Chem.)* **1989**, *30*, 115. (g) Padias, A. B.; Hall, H. K.; Tomalia, D. A. *Polym. Prepr. (Am. Chem. Soc., Div. Polym. Chem.)* **1989**, *30*, 119. (h) Tomalia, D. A.; Naylor, A. M.; Goddard, W. A., III. *Angew Chem., Int. Ed. Engl.* **1990**, *29*, 138. (i) Tomalia, D. A.; Dewald, J. R. U.S. Patent 4 507 466, 1985; U.S. Patent 4 558 120, 1985; U.S. Patent 4, 568, 737, 1986; U.S. Patent 4, 587, 329, 1986; U.S. Patent 4, 631, 337, 1986; U.S. Patent 4, 694, 064, 1986; U.S. Patent 4, 857, 599, 1989.

(6) Moreno-Bondi, M.; Orellana, G.; Turro, N. J.; Tomalia, D. A. *Macromolecules* **1990**, *23*, 910.

(7) Gopidas, K. R.; Leheny, A. R.; Caminati, G.; Turro, N. J.; Tomalia, D. A. *J. Am. Chem. Soc.* **1991**, *113*, 7335.

(8) Caminati, G.; Turro, N. J.; Tomalia, D. A. *J. Am. Chem. Soc.* **1990**, *112*, 8515.

(9) Caminati, G.; Gopidas, K. R.; Leheny, A. R.; Turro, N. J. *Polym. Prepr. (Am. Chem. Soc., Div. Polym. Chem.)* **1991**, *32*, 602.

(10) Turro, C.; Niu, S.; Bossmann, S. H.; Tomalia, D. A.; Turro, N. J. *J. Phys. Chem.* **1995**, *99*, 5512.

(11) Ottaviani, M. F.; Cossu, E.; Turro, N. J.; Tomalia, D. A. *J. Am. Chem. Soc.* **1995**, *117*, 4387.

(12) (a) Ottaviani, M. F.; Turro, N. J.; Jockusch, S.; Tomalia, D. A. *J. Am. Chem. Soc.*, submitted for publication. (b) Ottaviani, M. F.; Turro, N. J.; Jokusch, S,; Tomalia, D. A. *Colloids Surf.*, submitted for publication.

(13) Ottaviani, M. F.; Bossmann, S.; Turro, N. J.; Tomalia, D. A. *J. Am. Chem. Soc.* **1994**, *116*, 661.

(14) Ottaviani, M. F.; Montalti, F.; Turro, N. J.; Tomalia, D. A. *J. Am. Chem. Soc.*, submitted for publication.

(15) (a) Kalyanasundaram, K. *Photochemistry in Microheterogeneous Systems*; Academic Press: Orlando, FL, 1987. (b) Thomas, J. K. *The Chemistry of Excitation at Interfaces*; ACS Monograph Series; American Chemical Society: Washington, DC, 1984 and references therein.

(16) (a) Meisel, D.; Matheson, M. S. *J. Am. Chem. Soc.* **1977**, *99*, 6577. (b) Meyerstein, D.; Rabani, J.; Matheson, M. S.; Meisel, D. *J. Phys. Chem.* **1978**, *82*, 1879. (c) Meisel, D.; Rabani, J.; Mayerstein, D.; Matheson, M. S. *J. Phys. Chem.* **1978**, *82*, 985. (d) Sassoon, R. E.; Rabani, J. *J. Phys. Chem.* **1980**, *84*, 1319. (e) Kelder, S.; Rabani, J. *J. Phys. Chem.* **1981**, *85*, 1637. (f) Duveneck, G. L.; Kumar, C. V.; Turro, N. J.; Barton, J. K. *J. Phys. Chem.* **1988**, *92*, 2028.

(17) (a) Kumar, C. V.; Barton, J. K.; Turro, N. J. *J. Am. Chem. Soc.* **1985**, *107*, 5518. (b) Barton, J. K.; Goldberg, J. M.; Kumar, C. V.; Turro, N. J. *J. Am. Chem. Soc.* **1986**, *108*, 2081. (c) Pyle, A. M.; Rehmann, J. P.; Meshoyrer, R.; Kumar, C. V.; Turro, N. J.; Barton, J. K. *J. Am. Chem. Soc.* **1989**, *111*, 3051. (d) Friedman, A. E.; Chambron, J. C.; Sauvage, J. P.; Turro, N. J.; Barton, J. K. *J. Am. Chem. Soc.* **1990**, *112*, 4960. (e) Kelly, J. M.; Tossi, A. B.; McConnell, D. J.; Ohuigin, C. *Nucleic Acids Res.* **1985**, *13*, 6017. (f) Gorner, H.; Tossi, A. B.; Stradowski, C.; Schulte-Frohlinde, D. J. *Photochem. Photobiol. B* **1988**, 67. (g) Kirsch-De Mesmacker, A.; Orellana, G.; Barton, J. K.; Turro, N. J. *J. Photochem. Photobiol.* **1990**, *52*, 461.

(18) Meyer, T. J. *Pure Appl. Chem.* **1990**, *62*, 1003 and references therein.

(19) Naylor, A. M.; Goddard, W. A., III; Kiefer, G. E.; Tomalia, D. A. *J. Am. Chem. Soc.* **1989**, *111*, 2341.

(20) Sano, H.; Tachiya, M. *J. Chem. Phys.* **1981**, *75*, 2870.

(21) (a) *Spin Labeling. Theory and Applications*; Berliner, L. J., Ed.; Academic Press: New York, 1976, Vol. 1; 1979, Vol. 2. (b) *Biological Magnetic Resonance. Spin Labeling. Theory and Applications*; Berliner, L. J., Reuben, J., Eds.; Plenum Press: New York, 1989; Vol. 8.

(22) Ottaviani, M. F.; Ghatlia, N. D.; Turro, N. J. *J. Phys. Chem.* **1992**, *96*, 6075.

(23) Bossmann, S. H.; Ghatlia, N. D.; Turro, C.; Ottaviani, M. F.; Dürr, H.; Turro, N. J. Manuscript in preparation.

(24) Ottaviani, M. F.; Ghatlia, N. D.; Bossmann, S. H.; Barton, J. K.; Dürr, H.; Turro, N. J. *J. Am. Chem. Soc.* **1992**, *114*, 8946.

(25) Ottaviani, M. F.; Venturi, F. *J. Phys. Chem.*, in press

(26) Schneider, D. J.; Freed, J. H. In *Biological Magnetic Resonance. Spin Labeling. Theory and Applications*; Berliner, L. J., Reuben, J., Eds.; Plenum Press: New York, 1989; Vol. 8, p 1

(27) (a) Martini, G.; Ottaviani, M. F.; Ristori, S.; Lenti, D.; Sanguineti, A. *Colloids Surf.* **1990**, *45*, 177. (b) Bonosi, F.; Gabrielli, G.; Margheri, E.; Martini, G. *Langmuir* **1990**, *6*, 1769. (c) Ristori, S.; Ottaviani, M. F.; Lenti, D.; Martini, G. *Langmuir* **1991**, *7*, 1958. (d) Ristori, S.; Martini, G. *Langmuir* **1992**, *8*, 1937 (e) Martini, G.; Ottaviani, M. F.; Ristori, S. *Croat. Chim. Acta* **1992**, *65*, 471.

(28) Turro, C.; Niu, S.; Bossmann, S. H.; Barton, J. K.; Turro, N. J. *Inorg. Chim. Acta*, in press.

(29) (a) Martini, G.; Ottaviani, M. F.; Romanelli, M J. *Colloid Interface Sci.* **1983**, *94*, 105. (b) Romanelli, M.; Ottaviani, M. F.; Martini, G. *J. Colloid Interface Sci.* **1983**, *96*, 373. (c) Martini, G.; Ottaviani, M. F.; Romanelli, M *J. Colloid Interface Sci.* **1987**, *115*, 87. (d) Martini, G.; Ottaviani, M. F.; Ristori, S.; Visca, M. *J. Colloid Interface Sci.* **1989**, *76*, 128. (e) Martini, G.; Ottaviani, M. F.; Romanelli, M.; Kevan, L. *Colloids Surf.* **1989**, *178*, 271.

JP960120M